Catalysis Today 138 (2008) 162–168

Contents lists available at ScienceDirect

Catalysis Today

journal homepage: www.elsevier.com/locate/cattod

H_2 production through steam reforming of ethanol over Pt/ZrO_2, Pt/CeO_2 and $Pt/CeZrO_2$ catalysts

Sania M. de Lima [a], Adriana M. Silva [a], Ivna O. da Cruz [a], Gary Jacobs [b], Burtron H. Davis [b], Lisiane V. Mattos [a], Fábio B. Noronha [a,*]

[a] *Instituto Nacional de Tecnologia - INT, Av. Venezuela 82, CEP 20081-312, Rio de Janeiro, Brazil*
[b] *Center for Applied Energy Research, The University of Kentucky, 2540 Research Park Drive, Lexington, KY 40511, USA*

ARTICLE INFO

Article history:
Available online 23 July 2008

Keywords:
Fuel cell
Hydrogen production
Steam reforming of ethanol
Pt catalysts

ABSTRACT

The effect of the support nature and metal dispersion on the performance of Pt catalysts during steam reforming of ethanol was studied. H_2 and CO production was facilitated over Pt/CeO_2 and $Pt/CeZrO_2$, whereas the acetaldehyde and ethene formation was favored on Pt/ZrO_2. According to the reaction mechanism, determined by temperature-programmed desorption (TPD) and Diffuse Reflectance Infrared Spectroscopy (DRIFTS) analysis, some reaction pathways are favored depending on the support nature, which can explain the differences observed on the resulting product distribution.

1. Introduction

Recently, H_2-powered fuel cells have been proposed to be a major energy source that could contribute to reductions in the global dependence on fossil fuels, greenhouse gas emissions and atmospheric pollution. Steam reforming, partial oxidation and autothermal reforming have been used to produce H_2 for fuel cells from different feedstock. Ethanol is an interesting alternative for H_2 production since it would conceivably generate far less greenhouse gas emissions than conventional fuels. In the literature, there are a large number of studies on H_2 production from steam reforming (SR) of ethanol for fuel cells [1]. However, this technology exhibits some disadvantages such as formation of byproducts, which can affect the efficiency of fuel cells, and result in catalyst deactivation. Hence, the economic viability for the use of ethanol as a source of H_2 depends on the development of appropriate catalysts. We have reported that Pt/CeO_2 and $Pt/CeZrO_2$ catalysts were found to be excellent candidates as catalysts for fuel processors for PEM fuel cell applications based on the partial oxidation of ethanol, since they exhibited good stability and activity for this reaction [2,3]. The aim of the current work is to compare the performance of Pt/ZrO_2, Pt/CeO_2 and $Pt/CeZrO_2$ catalysts during steam reforming of ethanol. The effect of the support on the reaction mechanism was investigated by TPD and DRIFTS techniques.

2. Experimental

CeO_2 and ZrO_2 supports were prepared by calcination of $(NH_4)_2Ce(NO_3)_6$ and $Zr(OH)_4$ at 1073 K, respectively. $CeZrO_2$ support (Ce/Zr = 3) was synthesized following a co-precipitation method [3,4]. Pt (1.5 wt%) was added to the supports by incipient wetness impregnation with a solution of $H_2PtCl_6{\cdot}6H_2O$. Then, samples were calcined at 673 K.

The BET surface areas were measured using a Micromeritics ASAP 2000 analyzer by N_2 adsorption at liquid N_2 temperature. Oxygen storage capacity (OSC) analyses were carried out at 723 K in a reactor coupled to a quadrupole mass spectrometer. Pt dispersion was estimated through cyclohexane (HC) dehydrogenation reaction at 543 K, using a H_2/HC ratio of 13.0. The experimental conditions of OSC and HC dehydrogenation were previously described [4]. The TPD experiments of adsorbed ethanol were performed in the same equipment described for OSC measurements. Prior to TPD analyses, the samples were reduced under H_2 at 773 K for 1 h. Then, the system was purged with He at 773 K and cooled to room temperature. The adsorption of ethanol was made at room temperature, using an ethanol/He mixture. After adsorption, the catalyst was heated to 773 K under He. DRIFTS analyses were recorded using a Nicolet Nexus 870 spectrometer equipped with a DTGS-TEC detector. Samples were first reduced at 773 K for 1 h under H_2:He (1:1). The catalyst was purged in He at 773 K, prior to cooling in He to 313 K. The DRIFTS analysis was carried out by using an ethanol + water mixture containing a H_2O/ethanol ratio of 2.0. The spectra were recorded at 313–773 K.

---

* Corresponding author. Tel.: +55 21 2123 1177; fax: +55 21 2123 1051.
E-mail address: fabiobel@int.gov.br (F.B. Noronha).

0920-5861/$ – see front matter © 2008 Elsevier B.V. All rights reserved.
doi:10.1016/j.cattod.2008.06.014

Table 1
BET surface area and O_2 uptakes obtained for all catalysts

Samples	BET surface area (m^2/g)	O_2 consumption (μmol O_2/g cat)
Pt/ZrO_2	20	9
Pt/CeO_2	14	194
$Pt/CeZrO_2$	34	626

Steam reforming of ethanol was performed in a fixed-bed reactor at atmospheric pressure. Prior to reactions, the catalysts were reduced at 773 K and then purged under N_2 at the same temperature. All reactions were carried out at 773 K, using a H_2O/ethanol molar ratio of 2.0. The reactant mixture (N_2:H_2O:ethanol molar ratio = 17:2.0:1.0) was obtained by flowing two N_2 streams (30 ml/min) through each saturator containing ethanol and water separately. The saturators with ethanol and water were maintained at 291 and 320 K, respectively, to obtain a H_2O/ethanol molar ratio of 2.0. The space velocity used was 180,000 mL/g h. In order to follow the catalyst deactivation within a short period of time, a small amount of catalyst was used (20 mg). The reaction products were analyzed by gas chromatography (Micro GC Agilent 3000 A) containing two channels for dual thermal conductivity detectors (TCD) and two columns: a molecular sieve and a Poraplot U column.

3. Results and discussion

3.1. Catalysts characterization

The BET analysis showed that all catalysts presented low surface areas. The addition of Zr to ceria increased the surface area of the catalysts from 14 to 34 m^2/g (Table 1). The oxygen uptake measured for Pt/ZrO_2 catalyst was very low (Table 1). On the other hand, Pt/CeO_2 and $Pt/CeZrO_2$ exhibited a large O_2 consumption. Furthermore, the oxygen storage capacity of $Pt/CeZrO_2$ is considerably higher than Pt/CeO_2, indicating that the presence of the Zr increased the reducibility of CeO_2 support. The oxygen consumption obtained for CeO_2 support was associated with the ability of cerium to act as an oxygen buffer by storing/releasing O_2 due to the Ce^{4+}/Ce^{3+} redox couple. The presence of ZrO_2 strongly increases the density of oxygen vacancies of the support due to the high oxygen mobility of the CeO_2–ZrO_2 solid solution formed, which was previously identified by XRD data [4]. The platinum dispersions calculated from cyclohexane dehydrogenation for Pt/ZrO_2, Pt/CeO_2 and $Pt/CeZrO_2$ catalysts were 29, 48 and 22%, respectively.

3.2. Steam reforming of ethanol

The SR of ethanol over Pt/ZrO_2, Pt/CeO_2 and $Pt/CeZrO_2$ samples as a function of time on stream (TOS) was carried out at 773 K (Fig. 1a–c). The initial ethanol conversion decreased in the order: $Pt/CeO_2 > Pt/ZrO_2 > Pt/CeZrO_2$ catalyst. These results showed that the initial activity of the catalysts followed the same trend as that of the Pt dispersion, suggesting that ethanol conversion increases as Pt particle size decreases. In addition, the ethanol conversion significantly decreased at the beginning of the reaction test for each of the Pt/ZrO_2, $Pt/CeZrO_2$ and Pt/CeO_2 catalysts. A strong deactivation was also observed for Rh/CeO_2–ZrO_2 catalysts during steam reforming of ethanol, and attributed to deposition of carbonaceous species on the catalyst surface [5]. In order to study the nature of the carbon deposits formed that may contribute to catalyst deactivation, TPO and TPD experiments (not shown) were carried out over $Pt/CeZrO_2$ after running the reaction. The TPO profile exhibited two peaks at around 597 and 1030 K corresponding to CO_2 formation. Erdohelyi et al. [6] reported that the decrease of hydrogen selectivity during steam reforming of ethanol was due to an inhibiting effect caused by surface acetate species. Recently, Platon et al. [7] studied the deactivation of $Rh/Ce_{0.8}Zr_{0.2}O_2$ catalysts during low-temperature ethanol steam reforming. Transmission electron microscopy (TEM) analysis did not reveal any significant metal particle sintering or carbon deposits whereas thermogravimetric analysis (TGA) did not indicate the existence of an important build-up of carbonaceous deposits, which may be a contributing factor in the deactivation of the catalyst. The TPD profile of $Pt/CeZrO_2$ catalyst exhibited CO_2 desorption from 600 K with a maximum at 953 K. The absence of oxygen in the feed indicates that this peak is likely due to the decomposition of a reaction intermediate, such as acetate or carbonate species, adsorbed on the surface. This suggests that the catalyst deactivation is not due to carbon deposition, but it is likely associated with the presence of acetate or carbonate species on the catalyst surface. That is, a deactivation phenomenon appears to occur as a function of time on stream that inhibits turnover of acetate and/or carbonate. As such, build-up of these intermediate species appears to be symptomatic of catalyst deactivation.

Regardless of the catalysts used, H_2, CO_2, CH_4, CO, acetaldehyde and ethene were always formed. The selectivity to H_2 strongly decreased during the first 3 h TOS for Pt/ZrO_2 and $Pt/CeZrO_2$ catalysts. After that interval, H_2 was no longer detected for Pt/ZrO_2, while its selectivity remained relatively stable for the $Pt/CeZrO_2$ catalyst. In the case of Pt/CeO_2, the H_2 production remained practically constant during 2 h TOS. After that, the H_2 selectivity continuously decreased. Decreases in H_2 selectivity and ethanol conversion were accompanied by increases in acetaldehyde and ethene selectivities for all catalysts tested. Dömök et al. [8] also detected a decrease in H_2 selectivity and an increase in the acetaldehyde selectivity during SR over an alumina-supported Pt catalyst. Significant amounts of ethene were only detected for Pt/ZrO_2 catalyst, which is likely due to ethanol dehydration over the support. The selectivity to CO_2 increased for all catalysts during the reaction time. Moreover, CO production was only detected at the beginning of the reaction test for all catalysts. In fact, after 3 h TOS, CO was no longer detected. Fig. 1d displays the product distribution results at the same level of conversion (~40%, dry basis, 773 K) for all catalysts tested. The formation of H_2 and CO was favored over Pt/CeO_2 and $Pt/CeZrO_2$ catalysts, whereas Pt/ZrO_2 catalyst exhibited the highest production of acetaldehyde and ethene. Another observation was that the addition of Zr to CeO_2 decreased the H_2 and CO production and increased the acetaldehyde and ethene formation rates. These results suggest an important influence of the nature of the support on the resulting product distribution. Therefore, to better understand the correlation between catalytic performance and the properties of the support, the reaction mechanism was studied by TPD of ethanol and DRIFTS analysis.

3.3. TPD of ethanol and DRIFTS analysis

The TPD profiles obtained for Pt/ZrO_2, Pt/CeO_2 and $Pt/CeZrO_2$ catalysts are presented in Fig. 2. Ethanol desorption was detected at 390 K for all catalysts. Similar results have been reported for TPD of ethanol over supported metal catalysts [2]. Furthermore, small amounts of acetaldehyde and ethene only were detected around 300–750 K for Pt/ZrO_2 and $Pt/CeZrO_2$ catalysts. The acetaldehyde and ethene, observed around 500 K on supported metal catalysts, are formed by dehydrogenation and dehydration of ethanol, respectively [6]. At low temperatures, all the catalysts tested exhibited a significant peak for H_2 production (400–417 K) and a

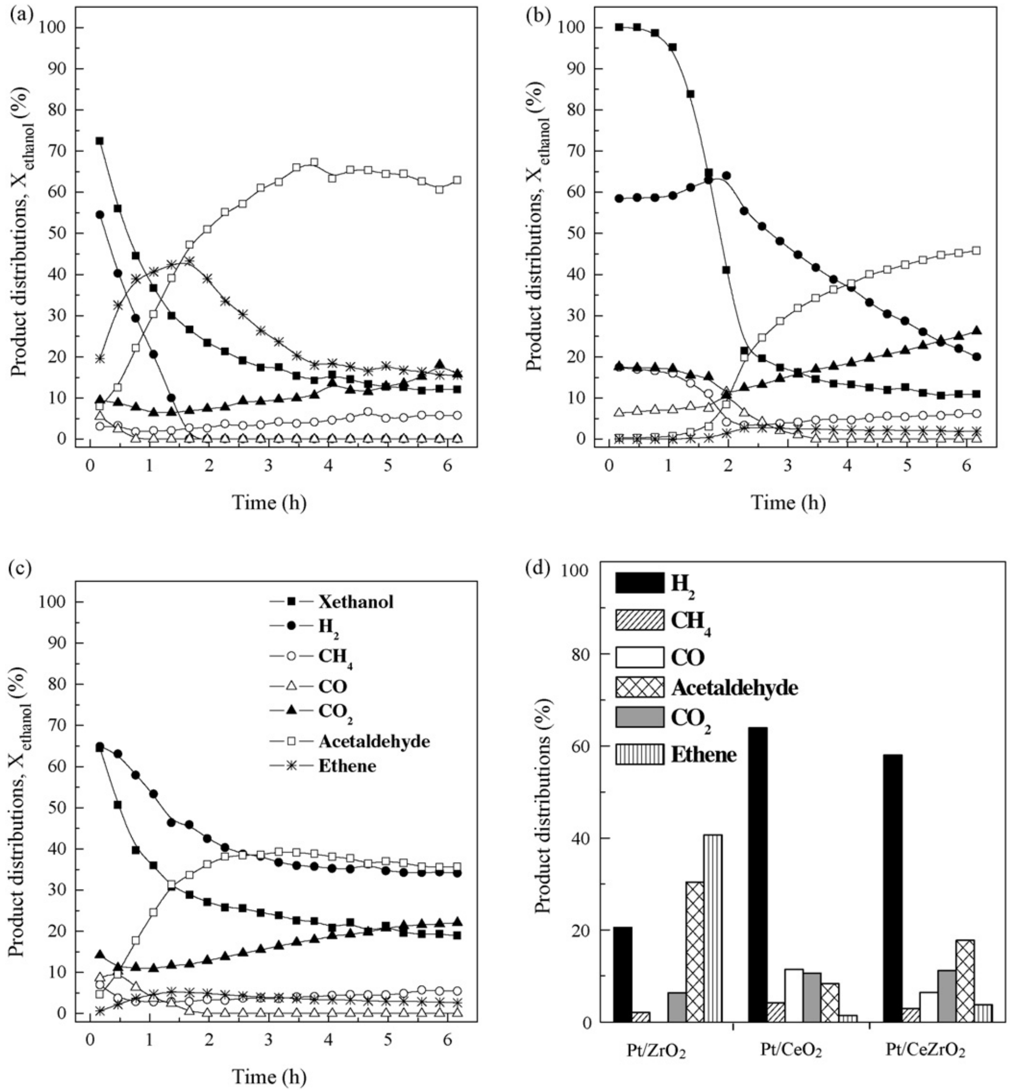

Fig. 1. Ethanol conversion obtained on SR of ethanol at 773 K for (a) Pt/ZrO_2; (b) Pt/CeO_2; (c) $Pt/CeZrO_2$ catalysts; (d) product distributions obtained at the same conversion (~40 %; 773 K) in dry basis.

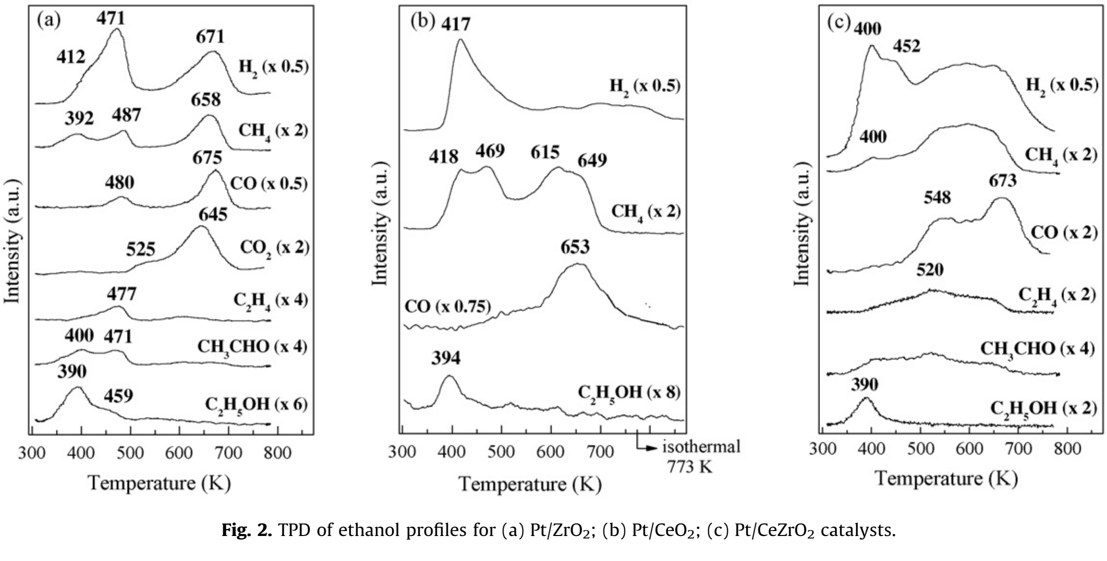

Fig. 2. TPD of ethanol profiles for (a) Pt/ZrO_2; (b) Pt/CeO_2; (c) $Pt/CeZrO_2$ catalysts.

smaller peak for CH_4 formation (398–418 K). H_2 and CH_4 formation were also detected around 450–470 K for all catalysts. In addition, Pt/ZrO_2 and Pt/CeO_2 catalysts exhibited a peak at 480 K and a shoulder at around 490 K, respectively, corresponding to CO formation. Some authors reported the formation of H_2, CH_4 and CO in the low-temperature region during TPD of ethanol over CeO_2-supported metals [2]. They suggested that ethanol adsorbs on the catalyst surface as ethoxy species that can be decomposed to H_2, CH_4 and CO by the metal function. However, in this work, the CO desorption at low temperatures was not observed, which suggests that CO still remained adsorbed on the catalyst surface in this temperature region.

At high temperatures, H_2, CH_4 and CO were detected for all catalysts. For Pt/ZrO_2 catalyst, peaks related to H_2, CH_4 and CO were observed at around 670 K. In addition, a broad peak for H_2 production between 600 and 773 K and two peaks associated with CH_4 formation at 615 and 649 K were also detected. Concerning CO formation over Pt/CeO_2 catalyst, a peak at 653 K was observed. For Pt/$CeZrO_2$ catalyst, the TPD profiles presented two broad peaks (between 500 and 700 K) related to both H_2 and CH_4 formation, whereas CO desorption was detected at 548 and 673 K. It is important to stress that CO_2 formation was only detected for the Pt/ZrO_2 catalysts at 525 and 645 K. No significant production of crotonaldehyde, acetone or benzene was observed by TPD analysis. The formation of CO and CH_4 at high temperatures (above 500 K) during TPD of ethanol over CeO_2 support has been assigned to the products of decomposition of carbon species previously formed (e.g., acetaldehyde, acetate species) [2]. According to them, a fraction of acetate species can be oxidized to carbonate species that are decomposed to CO_2. It was also observed that the amount of CO_2 desorbed from alumina was higher than that observed over ceria support [2]. According to the literature [4], CO_2 can replenish the oxygen vacancies of the CeO_2 support, releasing CO as a product. Since alumina does not have oxygen vacancies, it follows that the CO_2 formation rate is likely higher over this support. In the present work, the OSC analysis showed that Pt/CeO_2 and Pt/$CeZrO_2$ catalysts exhibited a high density of oxygen vacancies, which can explain the absence of CO_2 and the large desorption peak assigned to CO at high temperatures during TPD experiments. Finally, the production of H_2 detected at high temperature in the TPD profiles of all catalysts could be assigned to the desorption of H_2 previously formed during the different steps of ethanol dehydrogenation.

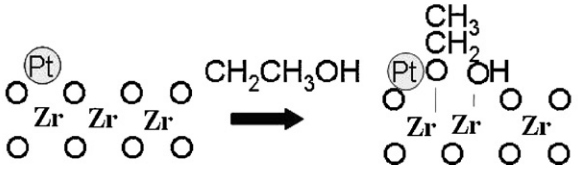

Scheme 1. Activation of ethanol on Zr^{4+} cations by ethoxy formation.

Reduction of Pt/CeO_2, Pt/ZrO_2, and Pt/$CeZrO_2$ catalysts in hydrogen leads to the formation of Type II bridging OH groups on the oxide surface via the dissociation of H_2 on Pt and spill over to the oxide surface [9]. The sites can be visualized to be O-vacancy defect sites associated with dissociated H_2O. Actually, TPR profiles of ceria-based catalysts revealed that surface ceria is completely reduced to Ce^{3+} below 700 K [4]. The lower extent of reduction of Pt/ZrO_2, as quantified by oxygen titration, suggests that these defect sites are lower in surface concentration and likely confined to the region in close proximity to Pt particles.

The DRIFTS spectrum obtained on the Pt/ZrO_2 catalyst at room temperature (Fig. 3) exhibited bands at 1051, 1088, 1450, 1538, 1637, 2062, 2898 and 2978 cm^{-1}. The bands at 1051, 1088, 2898 and 2978 cm^{-1} are related to different vibrational modes of ethoxy species (1051 and 1088 cm^{-1}: ν(CO); 2898 cm^{-1}: $\nu_s(CH_3)$; 2978 cm^{-1}: $\nu_a(CH_3)$), which were formed by dissociative adsorption of ethanol [2,10–12]. Since the reducibility of the ZrO_2 support is very low, ethanol will likely dissociate to CH_3CH_2O– and H– over zirconia sites whereby the Zr atoms involved are unsaturated Zr^{4+} (Scheme 1). The bands at 1538, 1450 and 1419 cm^{-1} can be attributed to the ν_a(OCO), $\delta_a(CH_3)$ and ν_s(OCO) vibrational modes of acetate species, respectively [13]. Therefore, a fraction of the ethoxy species react to form acetate species, most likely via addition of O from adsorbed –OH species (Scheme 2). The band at 1637 cm^{-1} is related to the ν(CO) vibrational mode of acetyl species. It has been suggested that a fraction of the ethoxy species is dehydrogenated to acetaldehyde, which may be further dehydrogenated to acetyl species [14]. Finally, the band at 2062 cm^{-1} has been attributed to the ν(CO) vibrational modes of linearly adsorbed CO on metal particles [2]. The formation of CO at low temperatures has also been attributed previously to the decomposition of ethoxy species [2]. When the temperature was

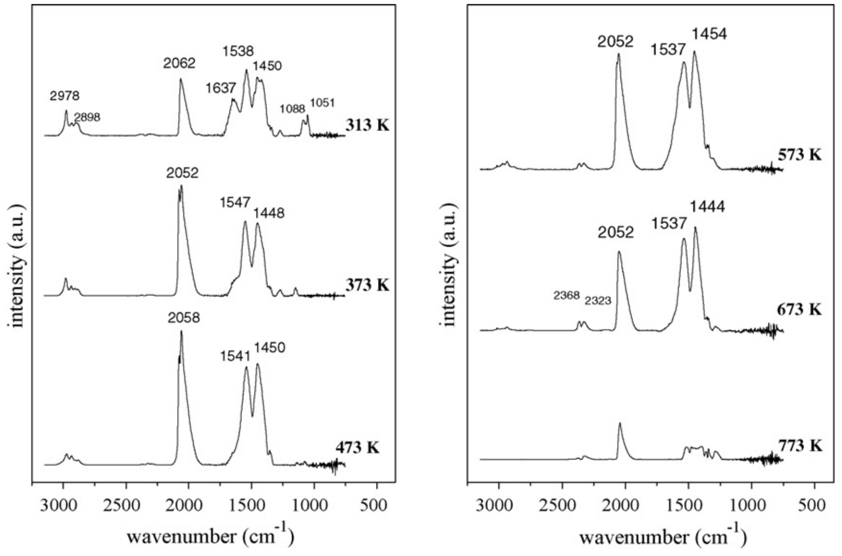

Fig. 3. DRIFTS spectra at different temperatures and under ethanol + water obtained on Pt/ZrO_2 catalyst.

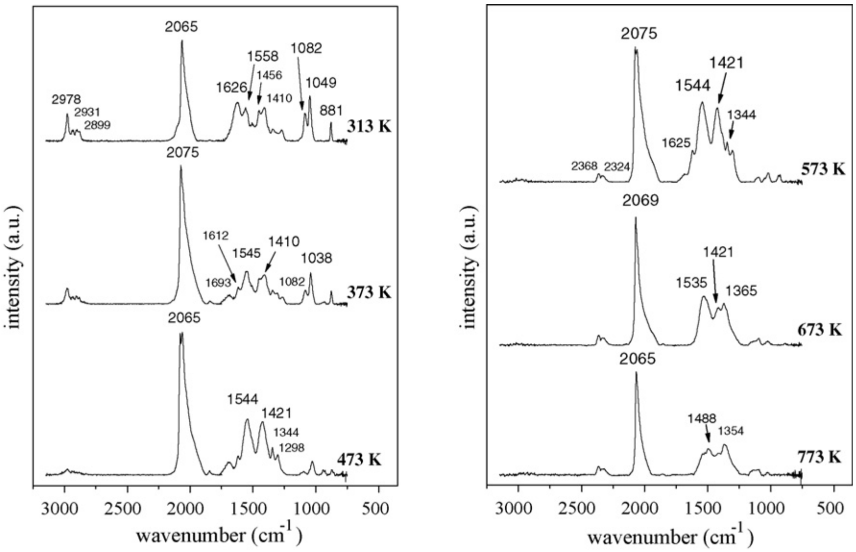

Fig. 4. DRIFTS spectra at different temperatures and under ethanol + water obtained on Pt/CeO$_2$ catalyst.

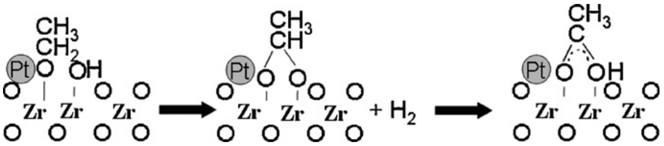

Scheme 2. Transformation of ethoxy species to acetate species via addition of O from adsorbed –OH species.

increased from 313 to 473 K, the bands corresponding to ethoxy and acetyl species disappeared and the intensity of the bands assigned to acetate species and adsorbed CO increased. At 573 K, the bands related to acetate species and adsorbed CO remained unchanged. In addition, the bands characteristic of CO$_2$ (2368 and 2323 cm^{-1}) were now present. The production of CO$_2$ can be assigned to the decomposition of acetate species via carbonate species [2]. This forward acetate decomposition should also result in the evolution of methane. Above 573 K, the bands assigned to CO$_2$ formation slightly increased and the bands related to adsorbed CO and acetate species decreased.

The DRIFTS spectrum obtained for Pt/CeO$_2$ catalyst at room temperature (Fig. 4) exhibited the formation of similar species observed for the Pt/ZrO$_2$ catalyst: ethoxy species (1049, 1082, 1450, 2899 and 2978 cm^{-1}); acetyl species (1626 cm^{-1}); acetate species (1410 and 1558 cm^{-1}); adsorbed CO (2065 cm^{-1}). However, it is important to stress that the Pt/CeO$_2$ catalyst exhibited a higher extent of reduction, which should lead to a high density of Type II bridging OH groups associated with O-vacancy defect sites. Therefore, the route involving Type II bridging OH groups is likely the main pathway to the formation of acetate species for this catalyst (Schemes 3 and 4). At 373 K, the bands assigned to ethoxy and acetyl species decreased whereas the bands corresponding to adsorbed CO increased. In addition, no significant changes were observed in the intensity of the bands related to acetate species. Increasing temperature to 573 K increased the formation of acetate species, while the intensity of the bands assigned to adsorbed CO remained constant. At this temperature, the bands due to ethoxy species completely disappeared whereas the bands corresponding to CO$_2$ formation are now detected. Further increase of temperature reduced the intensity of the bands assigned to acetate species and adsorbed CO.

In the case of Pt/CeZrO$_2$ catalyst (Fig. 5), the species formed at room temperature were also similar to those obtained on Pt/ZrO$_2$ and Pt/CeO$_2$ catalysts. Furthermore, the reaction pathway of acetate formation involving Type II bridging OH groups (Schemes 3 and 4) seems to be very important on Pt/CeZrO$_2$ catalyst, since CeZrO$_2$ support exhibited the highest reducibility. The addition of zirconium to ceria strongly increased the density of oxygen vacancies of the support due to the high oxygen mobility of the CeO$_2$–ZrO$_2$ solid solution formed, which was also identified by XRD analysis. Therefore, the density of Type II bridging OH groups formed on the oxide surface after reduction should follow the same

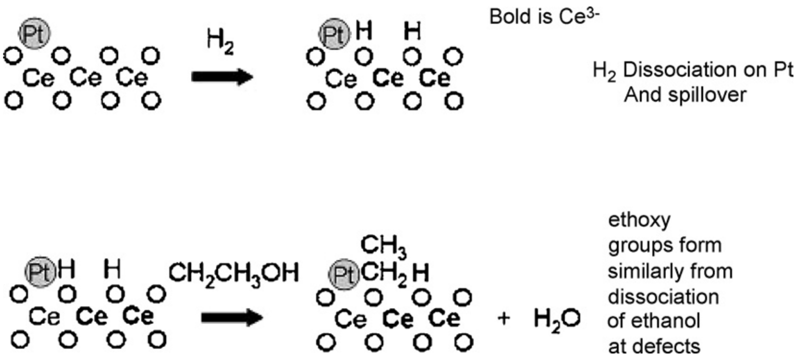

Scheme 3. Activation of ethanol on Ce^{3+} cations by ethoxy formation.

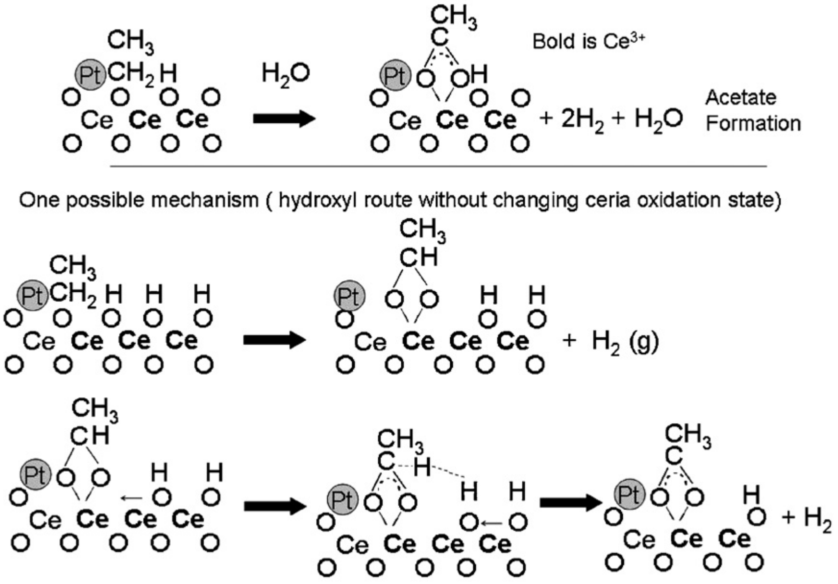

Scheme 4. Transformation of ethoxy to acetate species by Type II bridging OH groups.

OSC order. This means that Pt/ZrO_2 catalyst should exhibit the lowest surface concentration of these defect sites, which should be restricted to the region in close proximity to Pt particles. Therefore, the conversion of the dehydrogenated species to acetate species should preferentially follow Scheme 2, where the intermediate reacts with oxygen from the support. In the case of Pt/CeO_2 and $Pt/CeZrO_2$ catalysts, the acetate species could be formed via either/both schemes proposed. We also carried out XPS analysis of the reduced Pt/CeO_2, Pt/ZrO_2 and $Pt/Ce_xZr_{1-x}O_2$ catalysts [15]. The Ce/Zr ratio of the reduced $Pt/Ce_{0.75}Zr_{0.25}O_2$ catalyst (12.0) was significantly different from the nominal Ce/Zr ratio (3.0). This result reveals a strong cerium oxide surface segregation. Therefore, the surface of the support contains mainly cerium atoms and then ethanol adsorbs basically over Ce^{3+} cations. The main role of zirconium is to improve the oxygen mobility and the concentration of oxygen vacancies, which will favor the reaction pathway via the conversion of ethoxy to acetate species involving Type II bridging OH groups through Scheme 3.

Increasing temperature to 373 K increased the intensity of the bands due to acetate species and adsorbed CO while the ethoxy species and acetyl species decreased. The spectrum at 473 K is dominated by very intense bands related to acetate species and adsorbed CO. Gas phase CO_2 is clearly detected at 573 K. Above 673 K, the intensities of the bands characteristics of acetate species and adsorbed CO strongly decreased.

A comparison of the DRIFTS spectra obtained on all catalysts showed that, in spite of the presence of the same species, there are significant differences in the relative intensities of the bands corresponding to each species, which may in turn reflect on the selectivities of reaction pathways. At room temperature, the ratio between the intensity of acetate species and ethoxy species (acetate/ethoxy ratio) decreased in the order: $Pt/ZrO_2 \gg Pt/CeO_2 > Pt/CeZrO_2$, which suggests that the transformation of ethoxy to acetate appears to be favored over the Pt/ZrO_2 catalyst. On the other hand, the Pt/CeO_2 catalyst exhibited the lowest acetate/adsorbed CO ratio ($Pt/ZrO_2 > Pt/CeZrO_2 > Pt/CeO_2$) at

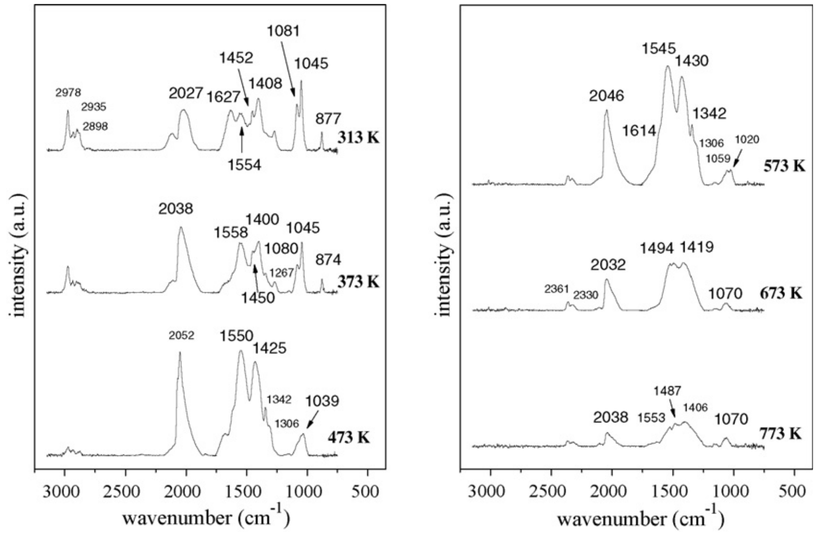

Fig. 5. DRIFTS spectra at different temperatures and under ethanol + water obtained on $Pt/CeZrO_2$ catalyst.

room temperature, which appears to reflect the higher Pt dispersion. This result suggests that the decomposition of ethoxy species to CO, CH_4 and H_2 is facilitated over Pt/CeO_2 catalyst. At high temperatures, the acetate/adsorbed CO ratio decreased in the order: Pt/$CeZrO_2$ > Pt/ZrO_2 > Pt/CeO_2, which indicates that the decomposition of acetate was favored over the CeO_2-based catalyst. These results can explain the highest formation of H_2, CH_4 and CO during SR of ethanol at 773 K for the Pt/CeO_2 catalyst. Forward acetate decomposition is likely an important step in generating CH_4 and CO_2 products, just as forward-formate decomposition is proposed to be important for water–gas shift. The latter reaction is found to be facile over O-vacancy defect-laden oxides in combination with a metal, like Pt. In water–gas shift, the O-vacancy defects on ceria promote the activation of H_2O to form Type II bridging OH groups that react with CO to produce formate. Forward-formate decomposition is promoted by both steam and Pt, the latter of which assists in dehydrogenating the formate molecule and resulting in carbonate formation. In an analogous manner, the steam reforming of ethanol, which involves acetate instead of formate, should therefore be promoted by both steam and Pt, the latter of which should assist in demethanating the acetate molecule, also resulting in carbonate formation [16]. While carbonate decomposes to CO_2, the CO_2 will in turn react via reverse water–gas shift to produce CO. However, it is also suggested by the results that the support plays a pivotal role in governing selectivity. The ZrO_2 support, which only exhibits very limited reduction, favored a higher selectivity to the dehydration product, ethene, which is a reaction characteristic of the support.

4. Conclusions

The support nature significantly affected the product distribution obtained on SR of ethanol over supported Pt catalysts. The H_2 and CO formation was favored over Pt/CeO_2 and Pt/$CeZrO_2$ catalyst, whereas, Pt/ZrO_2 catalyst exhibited the highest production of acetaldehyde and ethene. These results are explained by a reaction mechanism determined by TPD and DRIFTS analysis. At low temperature, acetate formation is favored over the Pt/ZrO_2 catalyst whereas the ethoxy decomposition to CO, CH_4 and H_2 is facilitated over Pt/CeO_2 catalyst. At high temperature, the forward acetate decomposition is promoted by both steam and Pt and is favored over the CeO_2-based catalyst. These results are likely due to the higher Pt dispersion on Pt/CeO_2 catalyst.

Acknowledgements

The authors wish to acknowledge the financial support from CNPq, CTENERG/FINEP (01.04.0525.00) and Commonwealth of Kentucky.

References

[1] P.D. Vaidya, A.E. Rodrigues, Ind. Eng. Chem. Res. 45 (2006) 6614.
[2] L.V. Mattos, F.B. Noronha, J. Catal. 233 (2005) 453.
[3] L.V. Mattos, F.B. Noronha, J. Power Sources 145 (2005) 10.
[4] F.B. Passos, E.R. Oliveira, L.V. Mattos, F.B. Noronha, Catal. Today 101 (2005) 23.
[5] H. Roh, A. Platon, Y. Wang, D.L. King, Catal. Lett. 110 (2006) 1.
[6] A. Erdohelyi, J. Raskó, T. Kecskés, M. Tóth, M. Dömök, K. Baán, Catal. Today 116 (2006) 367.
[7] A. Platon, H.S. Roh, D.L. King, Y. Wang, Top. Catal. 46 (2007) 374.
[8] M. Dömök, M. Tóth, J. Raskó, A. Erdohelyi, Appl. Catal. B 69 (2007) 262.
[9] C. Binet, M. Daturi, J.C. Lavalley, Catal. Today 50 (1999) 207.
[10] A. Yee, S.J. Morrison, H. Idriss, J. Catal. 191 (2000) 30.
[11] A. Yee, S.J. Morrison, H. Idriss, Catal. Today 63 (2000) 327.
[12] J. Rasko, A. Hancz, A. Erdohelyi, Appl. Catal. A 269 (2004) 13.
[13] A. Yee, S.J. Morrison, H. Idriss, J. Catal. 186 (1999) 279.
[14] H. Idriss, C. Diagne, J.P. Hindermann, A. Kiennemann, M.A. Barteau, J. Catal. 155 (1995) 219.
[15] F.B. Noronha, E.C. Fendley, R.R. Soares, W.E. Alvarez, D.E. Resasco, Chem. Eng. J. 82 (2001) 21.
[16] G. Jacobs, R.A. Keogh, B.H. Davis, J. Catal. 245 (2007) 326.